

# Airflow to disperse refrigerant leaks from hydrocarbon refrigeration systems <sup>1</sup>

D. Colbourne<sup>(a)\*</sup>, K. O. Suen<sup>(b)</sup>

<sup>(a)</sup> Re-phridge Ltd, c/o GIZ Proklima and Deutsche Umwelthilfe e.V.

<sup>(b)</sup> University College London, Gower Street, London, WC1E 6BT, UK

## Highlights

- Theoretical and experimental characterisation of the dilution process of leaks in indoor unit airflow.
- Formulae to determine minimum indoor unit airflow to dilute leaks to below LFL.
- Measurements to examine dilution of stratified layer of refrigerant-air mixture in room.
- Methodology developed to determine response time and leak rate for initiating airflow.

## Abstract

Whilst R290 is currently used to a limited extent in room air conditioners there is a desire for wider application due to its excellent performance and negligible global warming potential. The product standard IEC 60335-2-40 specifies requirements to limit the allowable refrigerant charge in such a way that it obstructs the wider use of R290. Airflow of an indoor unit can be used to dilute a refrigerant leak, enabling substantially greater charge quantities to be used. A numerical model based on entrainment theory was developed and supported by analysing the behaviour of experimentally simulated releases under various conditions with indoor unit airflow. The work determines the minimum airflow rate necessary to prevent formation of a flammable concentration within the room. Further, the work includes determination of appropriate response time and leak rate to initiate airflow once a leak has begun. The developed methodology can equally be applied to commercial refrigeration units and other flammable refrigerants.

## Keywords

Hydrocarbon refrigerant, concentration, safety, air conditioner, indoor unit airflow, R290

\* Corresponding author; Tel: +44 1789 268 285; email: dc@re-phridge.co.uk

## Nomenclature

### Abbreviations

AC	air conditioner
CFD	computational fluid dynamics
CRU	commercial refrigeration unit
HC	hydrocarbon refrigerants
IDU	indoor unit

---

<sup>1</sup> An extension of Colbourne and Suen (2018a).

IEC	International Electrotechnical Commission
IPA	Initiation period for airflow
LFL	lower flammability limit
MSLR	Maximum safe leak rate
NE	negligible extent (zone of)
RACS	room air conditioning system

### Symbols

$a_1, a_2$	constants [-]
$A_o$	area of jet discharge opening [m <sup>2</sup> ]
$A_{rm}$	room floor area [m <sup>2</sup> ]
$Ar_o$	Archimedes number based on discharge conditions [-]
$b$	a constant [-]
$C$	refrigerant concentration [kg m <sup>-3</sup> ]
$C_f$	floor concentration [kg m <sup>-3</sup> ]
$C_{f,max}$	maximum floor concentration at beginning of the release [kg m <sup>-3</sup> ]
$C_{f,max,t}$	maximum floor concentration at cessation of the release [kg m <sup>-3</sup> ]
$C_o$	refrigerant concentration at discharge [kg m <sup>-3</sup> ]
$\bar{C}_{sur,t}$	average concentration of the surrounding air at cessation of the release [kg m <sup>-3</sup> ]
$C(x)$	concentration at distance ( $x$ ) along a jet [kg m <sup>-3</sup> ]
$f(I)$	combination of volume, momentum, energy and buoyancy flux integrals [-]
$F$	concentration limit applied to the LFL [-]
$g$	gravitational constant [= 9.81 m s <sup>-2</sup> ]
$g'$	reduced gravity [m s <sup>-2</sup> ]
$h_l$	height of mixture layer [m]
$h_a$	height of centre of air discharge [m]
$h_o$	height of base of unit [m]
$h_{rm}$	room height [m]
$LFL_m$	lower flammability limit by mass [kg m <sup>-3</sup> ]
$m_{ACL}$	allowable charge limit of refrigerant [kg]
$\dot{m}_{leak}$	mass flow of refrigerant release [kg s <sup>-1</sup> ] or [g min <sup>-1</sup> ]
$\dot{m}_{MSLR}$	mass flow of maximum safe leak rate [kg s <sup>-1</sup> ]
$m_r$	mass of refrigerant released [kg]
$\dot{m}_{suct,t}$	mass flow of refrigerant into the IDU suction at cessation of the release [kg s <sup>-1</sup> ]
$\dot{m}_{sur,t}$	entrained mass flow of refrigerant from room/surroundings at cessation of the release [kg s <sup>-1</sup> ]
$P$	perimeter around the flow field [m]
$Q$	nominal cooling capacity [kW]

$R$	coefficient for heterogeneity of discharged refrigerant-air [-]
$t$	time of release cessation from start of release [s]
$t_{dp}$	time for mixture plume to descend from IDU to floor [s]
$t_{IDU}$	time for release to emerge from the IDU, when considering IPA and MSLR [s]
$t_{IPA}$	time for IPA [s]
$t_{pf}$	time for mixture to propagate across floor until forming a volume of negligible extent [s]
$\bar{u}_{pf}$	average front propagation speed [ $\text{m s}^{-1}$ ]
$\bar{u}_c$	centreline velocity along $x$ direction [ $\text{m s}^{-1}$ ]
$u_o$	air velocity at discharge [ $\text{m s}^{-1}$ ]
$\dot{V}$	volume airflow rate [ $\text{m}^3 \text{s}^{-1}$ ]
$\dot{V}_{o,min}$	minimum discharge airflow rate [ $\text{m}^3 \text{s}^{-1}$ ]
$\dot{V}_o$	discharge airflow rate [ $\text{m}^3 \text{s}^{-1}$ ]
$\dot{V}_e$	entrained airflow rate [ $\text{m}^3 \text{s}^{-1}$ ]
$V_{NE}$	volume of mixture corresponding to negligible extent [ $\text{m}^3$ ]
$V_{rm}$	room volume [ $\text{m}^3$ ]
$x$	distance along the jet [m]
$x_T$	air throw, distance travelled until jet termination [m]

#### Greek symbols

$\alpha$	entrainment coefficient [-]
$\rho_a$	air density [ $\text{kg m}^{-3}$ ]
$\rho_m$	density of the refrigerant-air mixture [ $\text{kg m}^{-3}$ ]
$\vartheta$	an experimentally determined constant for MSLR [ $\text{s}^{-1}$ ]
$\varphi$	adjustment factor [-]
$\psi$	adaption coefficient [-]

## 1 Introduction

Hydrocarbon refrigerants (HC), such as R290, have excellent performance and negligible global warming potential. Within the context of the Kigali Amendment of the Montreal Protocol and national legislation there is a desire for their wider application. Thus, larger quantities of HC are needed for room air conditioning systems (RACS) than safety standards, such as IEC 60335-2-40 (2017), currently permit (Colbourne et al., 2020). A refrigerant leak from a RACS indoor unit (IDU), a substantial volume of refrigerant-air mixture should not build up which could potentially lead to fire or explosion. One measure to mitigate this is to use forced airflow from the IDU to disperse leaked refrigerant. IDUs normally have a set airflow rate as defined by the manufacturer to provide a given capacity, air throw, etc. and users may select from several incremental fan speed settings. It is desirable to identify whether the lowest airflow setting is adequate to dilute a leak or a higher airflow rate is needed, depending on whether the unit fan is already in

operation or is to be initiated by a detection system. The same approach can also be applied to commercial refrigeration units (CRU).

A formula is provided within IEC 60079-10-1 (2021) that can be transposed to calculate rate of extract ventilation (Colbourne and Suen, 2018a) intended to prevent formation of a flammable mixture. However, it assumes continuous release and replenishment of the room with fresh air; this does not represent RACS or CRU in a closed room. IEC 60335-2-40, clause GG.2.3.1, defines minimum airflow and discharge velocity for “A2L” refrigerants but it is primarily aimed at upwardly directed airflow (i.e., floor units) and does not deem the entire room volume available for mixing.

There are various studies where airflow is used to disperse leaks.

Jia et al. (2015) presented room concentration measurements for R32 and showed that the release was well mixed whilst the unit fan was operating. Jin et al. (2017) looked specifically at room ventilation on mixing of R32 leaks. Two cases were examined, one with outside air entering at the ceiling and exiting at the floor and another flowing in the opposite direction. Downward airflow (floor extraction) produced lower and more evenly mixed concentrations than with upwards (ceiling extraction) airflow.

Combining experiment and computational fluid dynamics (CFD) analysis of airflow dispersion, Hu et al. (2018) found that when airspeed at floor level was  $> 0.2 \text{ m s}^{-1}$ , it guaranteed avoidance of LFL at floor level. Air discharge angles were found to affect mixing, but as airflow rate increased the effect of discharge direction became indistinguishable.

Using CFD, Ram Prakash et al. (2021) examined the effect of room furniture, according to their size and distribution, on dispersion of R290 with IDU airflow. Across various scenarios, maximum concentration was found to increase by no more than about  $0.002 \text{ kg m}^{-3}$  (5% of LFL) relative to an empty room, demonstrating that peak concentrations are hardly affected even with highly congested rooms.

Whilst informative, the studies do not offer systematic methodologies to determine adequate airflow rate to minimise the possibility that flammable mixtures occur.

Unit airflow can be an effective means of mixing leaked refrigerant to avoid flammable concentrations and can enable greater charge quantities to be safely used in a room. A generalised approach is needed to determine minimum airflow rate, taking into account of the construction and installation characteristics of the equipment, as well as simplicity to apply. Thus, applicable principles for airflow mixing were adopted and applied to IDU and CRU characteristics. This led to the development of a general formula, which was examined experimentally and adjusted to account for empirical findings. Note it is specious to argue that zero risk is achievable (e.g., Colbourne and Suen, 2004), thus any approach cannot absolutely guarantee

against a flammable mixture forming, but to significantly reduce its chances of forming at potential ignition sources. Furthermore, it is impractical to employ excessively high airflow rates to account for the extremely low probability “worst case” scenarios.

Since a leak could occur when a fan is not operating, an approach is described to identify the initiation period for airflow (IPA), from the time at which a release begins to ensure already stratified mixture layers are quickly diluted. Given the potentially high cost for detecting very small leaks that do not pose significant flammability risk, a method is given to estimate the maximum safe leak rate (MSLR), being the threshold below which any leak could be considered relatively harmless and thus of airflow would be unnecessary.

## 2 Concept Development

When an air jet (e.g., from an IDU or CRU discharge grille) is blown into a free space, it entrains air from the surroundings so that its total volumetric airflow rate gradually increases (Figure 1). When the jet comprises a stream of released refrigerant, concentration of refrigerant within the flow field should correspondingly gradually decrease. A greater discharge volume flow rate will lead to a higher entrainment rate and hence more dilution.

For HCs that are denser than air, the “throw” will eventually terminate on the room floor (or at the opposite wall), depending upon whether the buoyancy or momentum effects of the jet dominate (Figure 1). The concentration at the termination location corresponds to the maximum floor concentration, before it further spreads and dilutes across the floor. If this maximum floor concentration is constrained to the lower flammability limit (LFL), then the corresponding minimum airflow rate can be determined. Derivation of a minimum airflow to prevent exceeding LFL on the floor, due to an assumed leak (expressed as release mass flow) is presented. The concept is developed on the basis of an IDU but is also evaluated with CRUs.

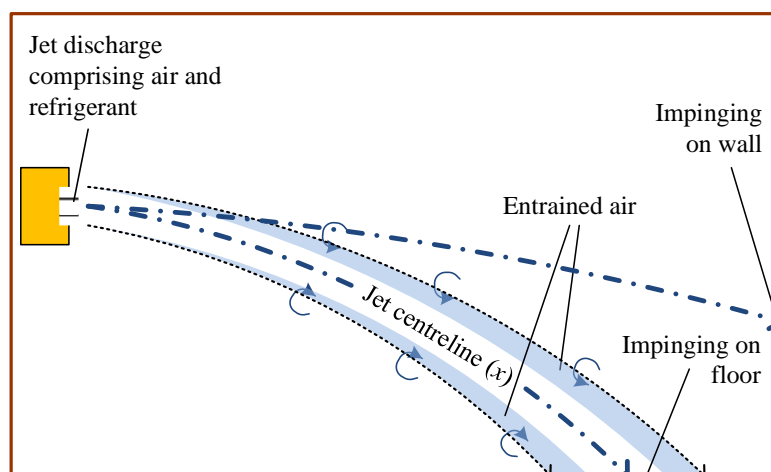


Figure 1: Schematic representation of entrainment process and “throw” termination

The analysis requires a number of assumptions: negligible air exchange between the room and environment, isothermal conditions, released refrigerant is predominantly vapour and denser than air, constant mass flow, negligible transit time for an element of the discharged mixture travelling from IDU to floor, and air discharge is horizontal.

## 2.1 Entrainment

Applying classical entrainment hypothesis (Morton et al., 1956; Turner, 1986), the rate of entrainment of surrounding fluid across a jet or plume boundary is proportional to the average centreline velocity and perimeter of the flow field (equation 1).

$$\frac{d\dot{V}(x)}{dx} = P\alpha\bar{u}_c \quad (1)$$

where  $\dot{V}(x)$  is volume flow rate,  $x$  is distance along the jet centreline,  $P$  is perimeter,  $\alpha$  is entrainment coefficient (typically assigned a value of around 0.1) and  $\bar{u}_c$  is centreline velocity along  $x$  direction. Etheridge and Sandberg (1996) derive closed equations for volume flow rate of buoyant jets at some distance from the jet exit. Their model for plane jets is adopted in this study (equation 2), as most IDUs have discharge openings with a high aspect ratio.

$$\dot{V}(x) = b\dot{V}_o\sqrt{\frac{\alpha x}{A_o}} \quad (2)$$

where the constant  $b = 2^{5/4}$  and  $A_o$  is the jet discharge opening area.

At distance  $x$  from the discharge, flow rate  $\dot{V}(x)$  is the sum of discharged airflow rate ( $\dot{V}_o$ ) plus additional airflow entrained. Therefore, total entrained airflow,  $\Sigma\dot{V}_e$  until distance  $x$  is equation (3).

$$\Sigma\dot{V}_e(x) = b\dot{V}_o\sqrt{\frac{\alpha x}{A_o}} - \dot{V}_o \quad (3)$$

## 2.2 Throw termination

It is taken that the negatively buoyant jet impinges on the floor first before reaching the opposite wall. From Etheridge and Sandberg, using constants for plane jet and setting identical boundaries for velocity and concentration fields (e.g., Doll et al., 2017), distance travelled until termination ( $x \rightarrow x_T$ ) is given as equation (4).

$$x_T = \left\{ h_a \frac{3.75A_o}{f(I)Ar_o b\sqrt{\alpha}} \right\}^{0.4} \quad (4)$$

where  $Ar_o$  is Archimedes number at the discharge,  $h_a$  is centre height of jet discharge and  $f(I)$  is a combination of volume, momentum, energy and buoyancy flux integrals determined analytically by Etheridge and Sandberg,  $f(I) = 0.39$ . Archimedes number at the IDU discharge condition is equation (5).

$$Ar_o = g' \frac{\sqrt{A_o}}{u_o^2} \quad (5)$$

where  $u_o (= \frac{\dot{V}_o}{A_o})$  is the IDU discharge velocity and  $g'$  is reduced gravity based on the mixture discharging into uncontaminated room air (equation 6).

$$g' = g \left( \frac{\rho_m - \rho_a}{\rho_a} \right) \quad (6)$$

where  $g$  is gravity,  $\rho_a$  is air density and  $\rho_m$  is density of the refrigerant-air mixture and can be approximated by  $\rho_m \cong C_o + \rho_a$ .  $C_o$  is the discharged airflow concentration (equation 7) and it is preliminarily assumed to be mixed homogeneously.

$$C_o = \frac{\dot{m}_{leak}}{\dot{V}_o} \quad (7)$$

Substituting equations (5), (6) and (7) into (4), yields equation (8).

$$x_T = \left\{ h_a \frac{9.6 \dot{V}_o^3 \rho_a}{g \dot{m}_{leak} A_o^{1.5} b \sqrt{\alpha}} \right\}^{0.4} \quad (8)$$

### 2.3 Dilution process

When the release begins and the jet, with an initial concentration of  $C_o$ , enters an uncontaminated space and refrigerant continues to mix with air homogeneously within the trajectory and expanding jet, concentration at distance ( $x$ ) can be expressed by equation (9):

$$C(x) = \frac{\dot{m}_{leak}}{V(x)} \quad (9)$$

As the release continues, refrigerant from the terminated jet mixes with the room air so the entrained air comprises an increasingly richer mixture, with average room air concentration peaking at cessation of the release (at time,  $t$ , i.e., release duration). The total volume of air entrained into the jet during the release, or the room air volume, whichever is smaller, is used to estimate average concentration of the surrounding air at  $t$  (equation 10).

$$\bar{C}_{sur,t} = \frac{m_r}{\min\{\Sigma \dot{V}_e t, V_{rm}\}} \quad (10)$$

where  $m_r$  is total mass of refrigerant released.

Numerically quantifying the term  $\Sigma \dot{V}_e t$  across a wide range of typical conditions, including airflow rate, release mass flow, room size, etc., showed that  $\Sigma \dot{V}_e t$  will always be larger than  $V_{rm}$  by up to a factor of five, indicating the mean room concentration  $\bar{C}_{sur,t}$  can be taken as  $\frac{m_r}{V_{rm}}$ .

When the release begins, maximum floor concentration ( $C_{f,max}$ ) corresponds to the jet concentration at  $x_T$  (equation 11).

$$C_{f,max} = \frac{\dot{m}_{leak}}{\dot{V}(x_T)} \quad (11)$$

Conditions may be that the jet impinges on the opposite wall, before the floor. For such cases,  $C_{f,max}$  is expected to be no higher than when the jet trajectories directly to the floor, since wall impingement will lead to further mixing before approaching the floor. Therefore, if the jet hits the wall first it is already covered by equation (11).

At  $t$ , the air along the trajectory of the jet will in addition comprise refrigerant entrained from the surroundings and drawn into the IDU suction. Thus,  $C_{f,max}$  will be equation (12).

$$C_{f,max,t} = \frac{\dot{m}_{leak} + \dot{m}_{sur,t} + \dot{m}_{suct,t}}{\dot{V}(x_T)} \quad (12)$$

where  $\dot{m}_{sur,t}$  is mass flow of refrigerant entrained from the surrounding air, equation (13).

$$\dot{m}_{sur,t} = \bar{C}_{sur,t} \Sigma \dot{V}_{e,t} \quad (13)$$

$\dot{m}_{suct,t}$  is mass flow of refrigerant drawn into the IDU suction, equation (14).

$$\dot{m}_{suct,t} = \bar{C}_{sur,t} \dot{V}_o \quad (14)$$

Substituting equations (13) and (14) into (12), yields equation (15).

$$C_{f,max,t} = \frac{\dot{m}_{leak}}{\dot{V}(x_T)} + \frac{m_r}{V_{rm}} \quad (15)$$

Introducing equation (2) into (15) and setting  $x = x_T$  enables  $C_{f,max,t}$  to be determined from IDU airflow (equation 16).

$$C_{f,max,t} = \frac{\varphi \dot{m}_{leak}}{Rb \dot{V}_o \sqrt{\frac{\alpha x_T}{A_o}}} + \frac{m_r}{V_{rm}} \quad (16)$$

where the two newly introduced parameters,  $R$  accounts for the discharged refrigerant-air heterogeneity and  $\varphi$  is an empirical adjustment factor; both are explained later.

## 2.4 Minimum airflow

By setting  $C_{f,max,t} = LFL_m$ , and rearranging equation (16) gives an explicit formula for minimum airflow rate, equation (17).

$$\dot{V}_{o,min} = \frac{\varphi \dot{m}_{leak}}{Rb \sqrt{\frac{\alpha x_T}{A_o}} \left( LFL_m - \frac{m_r}{V_{rm}} \right)} \quad (17)$$

Usually, refrigerant charge for RACS and CRU is determined according to the room size into which the equipment will be installed and the LFL, as equation (18) (Colbourne et al., 2020).



$$m_{ACL} = F \times LFL_m \times A_{rm} \times h_{rm} \quad (18)$$

where  $m_{ACL}$  is the allowable charge limit,  $h_{rm}$  is the room height, assumed 2.2 m to 2.5 m and  $F$  is a non-dimensional limit intended to prevent the entire room volume from approaching LFL.

$F$  represents the allowable charge per unit volume of the room and should be selected by the designer/manufacturer, depending upon how much refrigerant a system requires. Although it could be set as high as 0.99, to account for “noise factors” such as internal congestion, values not exceeding 0.5 should be used. Whilst a greater  $F$  represents a larger  $m_{ACL}$ , it also corresponds to higher airflow.

Equation (8) is inserted into equation (17) and to eliminate room volume, equation (18) is substituted in, whilst setting  $m_{ACL}$  as the maximum mass of refrigerant released ( $m_r$ ) and assuming  $h_{rm}$  to be 2.5 m. This yields equation (19).

$$\dot{V}_{o,min} = \frac{1.35\phi\sqrt{A_o}\dot{m}_{leak}^{3/4}}{Rh_a^{1/8}[LFL_m(1-F)]^{5/8}} \quad (19)$$

### 3 Measurements

Measurements of refrigerant concentrations were conducted to observe IDU discharge characteristics and provide data on lateral concentrations profiles within the room and additionally to refine the proposed formulae. Details of the equipment and laboratory setup are given in Colbourne and Suen (2021). Accuracy of electronic scales and mass flow meters used for releases are within  $\pm 1\%$  and gas sensors, which were recalibrated before and after each series of measurements, have an accuracy of  $\pm 3\%$ .

#### 3.1 IDU discharge heterogeneity

An initial assumption used in deriving the formulae (and for IEC 60335-2-40) was that a release is homogeneously mixed with the discharging airflow along the entire width of the IDU opening. Experiments using “floor” and “wall” type IDUs, both having an opening width of 1 m, were carried out to examine the validity of this assumption. R290 releases were made from different locations inside IDUs over a range of mass flow and airflow rates.

With the floor IDU, R290 concentrations were measured at six equidistant positions along the centreline of the air discharge, for a release at the right-hand return bends inside the IDU. Figure 2 indicates that irrespective of the flow rates, refrigerant predominantly remains within about one-third of the discharged air.

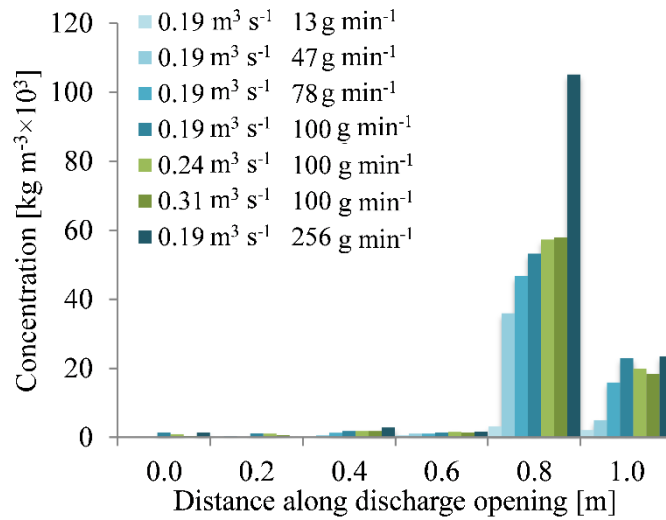


Figure 2: Measurements of R290 concentration at the discharge opening of a floor IDU for a release at the right-hand return bends

Other release locations were trialed, as indicated in Figure 3. Positioning and orientation of releases (as indicated by the arrows) were selected to create as much pre-mixing within the IDU as possible. Whilst some release positions led to a wider distribution of refrigerant, full homogeneity was never achieved.

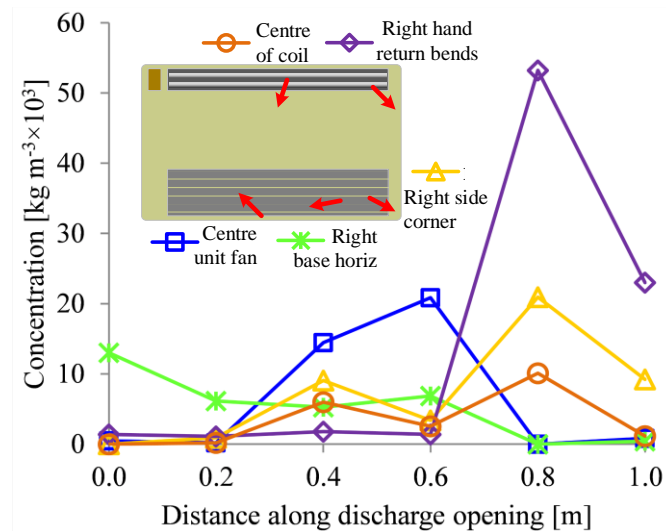


Figure 3: Concentration along air discharge arising from different release positions with  $0.19 \text{ m}^3 \text{ s}^{-1}$  airflow rate and  $100 \text{ g min}^{-1}$  release mass flow rate

Further measurements were carried out on wall IDUs, but with closer sampling points (40 mm apart) along the discharge opening, at five locations within the jet:  $0^\circ$  (horizontal),  $-23^\circ$ ,  $-45^\circ$ ,  $-67^\circ$  and  $-90^\circ$  (downward). Figure 4 shows R290 concentrations for airflow rates of  $0.13 \text{ m}^3 \text{ s}^{-1}$  and  $0.35 \text{ m}^3 \text{ s}^{-1}$  with  $30 \text{ g min}^{-1}$  release rate from the coil right-side return bends. A similar tendency to the floor IDU is seen, where most refrigerant exits along one-third of the length. Similar patterns were also seen in 2.5 kW and 8 kW IDUs, with alternate release locations and orientations near the return bends.

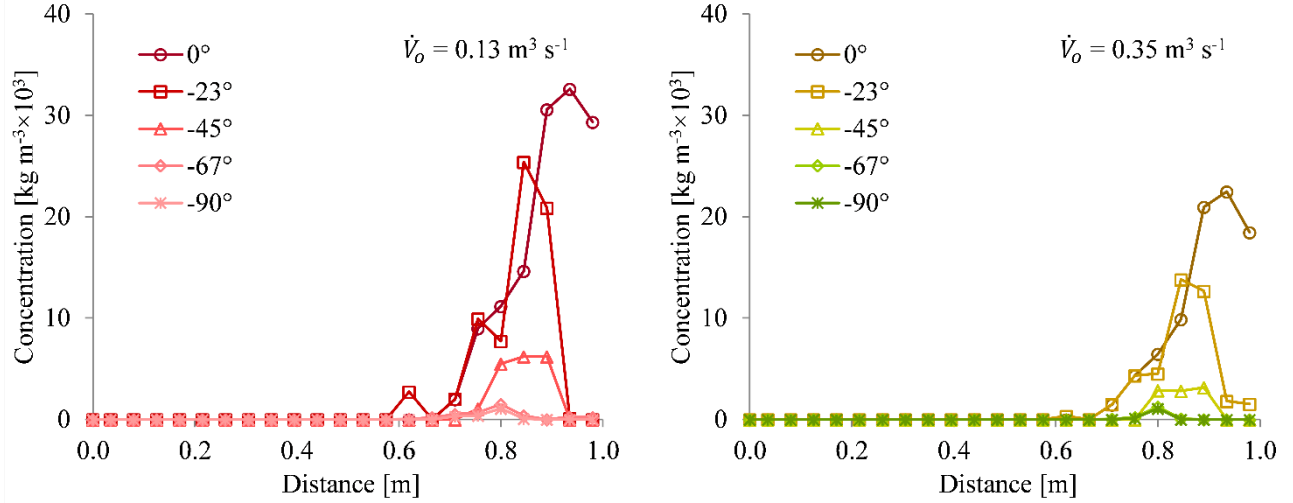


Figure 4: Measurements of R290 concentration at wall IDU discharge with  $30 \text{ g min}^{-1}$  release rate

Results for the floor and wall IDUs illustrate that changing airflow and release rate does not help homogenise the exit concentration but it does affect discharged concentration. The majority of airflow is not directly involved with dilution of the release and is far from homogeneous; two-thirds of discharged airflow may be neglected in relation to characterising the discharge conditions. Whilst the data in Figure 3, for example, show that refrigerant may be mixed in up to two-thirds of the discharged air, the most severe case (i.e., leading to highest  $C_f$ ) needs to be adopted. Thus, to account for the discharged refrigerant-air heterogeneity,  $R$  is to be set to  $\frac{1}{3}$ , and accordingly, this leads to requiring larger  $\dot{V}_{o,min}$ .

### 3.2 Spatial concentration profiles within the room

Measurements were made laterally across the room to establish the evolution of the jet concentration profile. Two sampling point arrangements (Colbourne and Suen, 2018a) were adopted.

(1) Sampling points spaced incrementally at 0.3 m apart along a single line on the floor from below the release point to the opposite wall of the room, in order to determine the location of  $x_T$ . Under various discharge conditions, Figure 5 plots local  $C_f$ , along with arrows indicating  $x_T$  (predicted from equation 8, where  $R = \frac{1}{3}$  has been applied to the actual airflow rate), which can be compared against  $x_T$  from the measurements (solid data points). There is fairly good agreement, with no more 0.5 m discrepancy.

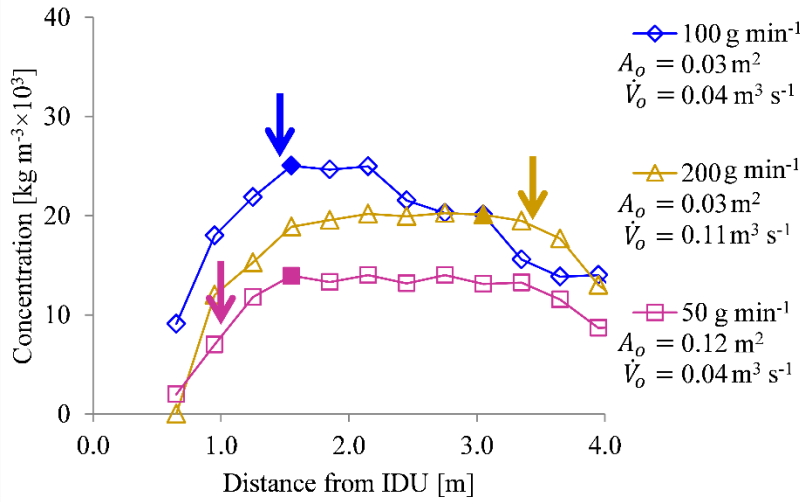


Figure 5: Measurements of floor concentrations at cessation of the release ( $t$ ) with release mass flow rates discharge, discharge opening area and airflow rate, to compare the experimental (solid data-points) and predicted (downward arrows) values of  $x_T$

(2) A matrix of three vertical planes, all aligned perpendicular to the front face of the IDU. The centre plane is aligned with the mid-point of the IDU discharge opening, with the other two  $\pm 0.6\text{m}$  on either side, with the  $+0.6\text{ m}$  plane aligned on the release point side. Each plane consists of six sampling points, with 3 of them positioned  $1\text{m}$  apart at the same height as the discharge opening (i.e.,  $1.5\text{ m}$  from floor, denoted “ $h_H$ ” in Figure 6) and another 3 sampling points directly below, at  $0.15\text{ m}$  from floor (denoted “ $h_L$ ”). Collectively, the 18 sampling points would provide a good indication of both the vertical and lateral distribution of the refrigerant within discharged air.

Results are shown for two airflow rates ( $0.35\text{ m}^3\text{ s}^{-1}$  and  $0.13\text{ m}^3\text{ s}^{-1}$ , Figure 6). Similar results are obtained for  $-0.6\text{m}$  plane (for brevity data not presented). Concentrations close to the release ( $+0.6\text{ m}$ ,  $h_H$ ) start at a high value and then decrease towards the room concentration at the far end of the room. Crucially, concentrations at  $h_L$  are found to be higher in the middle of the room (at  $1.5\text{ m}$ ), inferring a downward trajectory of the refrigerant-rich part of the jet. Results for the lower airflow rate suggest a steeper trajectory on account of the more pronounced decline in concentrations towards the far end of the room. By comparison, concentrations along the centre plane of the room, both at  $h_H$  and  $h_L$  are almost the same, representing the average room concentration. Since there is no variation from  $0.5\text{ m}$  to  $2.5\text{ m}$ , it demonstrates that the refrigerant-rich part of the jet at the  $+0.6\text{ m}$  plane is not spreading laterally across the discharged air. These observations support the flow process depicted in Figure 1 and further confirms the extension of the one-third lateral distribution of refrigerant along the throw of the air jet.

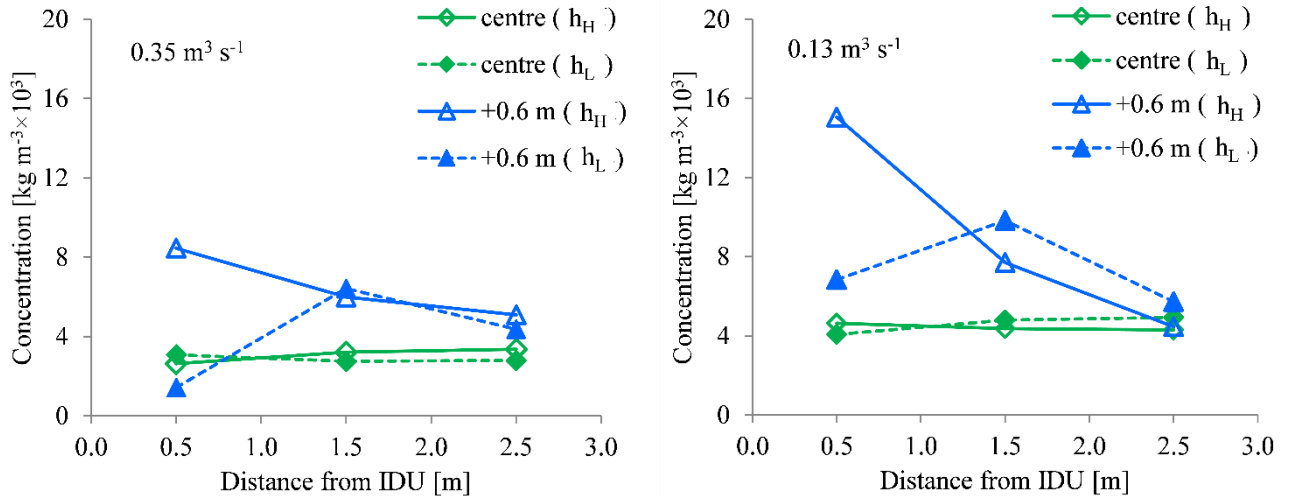


Figure 6: Local concentrations in front of air discharge;  $0.35 \text{ m}^3 \text{ s}^{-1}$ ,  $120 \text{ g min}^{-1}$  and  $0.2 \text{ kg}$ , and  $0.13 \text{ m}^3 \text{ s}^{-1}$ ,  $120 \text{ g min}^{-1}$  and  $0.2 \text{ kg}$

### 3.3 Application of formulations

$C_{f,max}$  from over 200 experiments, covering a wide range of conditions as listed in Table 1, were compared against the  $C_{f,max,t}$  predicted from equation (16) (where  $R = 1$ ), Figure 7 (left), showing half of the data-points are under-predicted.

Table 1: Range of variables across experiments

Variable	Range
Equipment types	RACS IDU (wall, floor, window, duct), CRU
Refrigerant	R290, R600a, CO <sub>2</sub>
Release mass	10 g – 2300 g
Release mass flow <sup>a</sup>	3 g min <sup>-1</sup> – 660 g min <sup>-1</sup>
Room area	10 m <sup>2</sup> – 45 m <sup>2</sup>
Room height	2.2 m – 3.5 m
Average concentration ( $m_r/V_{rm}$ )	0.0004 kg m <sup>-3</sup> – 0.034 kg m <sup>-3</sup>
Maximum floor concentration ( $C_{f,max}$ )	0.0004 kg m <sup>-3</sup> – 0.201 kg m <sup>-3</sup>
Airflow rate	0 m <sup>3</sup> s <sup>-1</sup> – 0.52 m <sup>3</sup> s <sup>-1</sup>
Air discharge velocity	0 m s <sup>-1</sup> – 10.6 m s <sup>-1</sup>
Air discharge height	< 0.1 m – 2.55 m
Release height	0.1 m – 2.5 m
Air discharge direction	-45° – +90°
Discharge opening area	0.01 m <sup>2</sup> – 0.17 m <sup>2</sup>

<sup>a</sup> Majority of leak holes lead to  $\dot{m}_{leak} < 15 \text{ g min}^{-1}$  and the largest  $< 150 \text{ g min}^{-1}$  (Colbourne et al., 2021b) so experimental  $\dot{m}_{leak}$  in this study were in excess of the likely leak size envelope.

However, the practical purpose of the eventual formula is to determine minimum airflow aimed at avoiding LFL at the floor. Therefore, in addition to setting  $R = \frac{1}{3}$ , an adjustment factor ( $\varphi$ ) is proposed to provide confidence that calculated  $\dot{V}_{o,min}$  from equation (19) would be high enough that  $C_{f,max}$  remains below LFL. Setting  $\varphi = 1.3$  in equation (16), over 90% of the data-points are shifted to the right of the line of equality (Figure 7, right), thus purposely “inflating” predicted  $C_{f,max,t}$ . The second term ( $\frac{m_r}{V_{rm}}$ ) in equation (16) has high certainty that is easily quantifiable, so no adjustment is deemed necessary.

All of the data-points could be moved to the right of the line of equality by setting a higher  $\varphi = 2.3$ , however, it would result in unnecessarily high airflow for the majority of RACHP equipment. Specifically, the cases remaining to the left of the line of equality are either low positioned ( $< 1$  m) IDUs with airflow discharged downwards or CRUs with floor-mounted condensers discharging mixture across the floor. These cases may warrant the higher  $\varphi$ . Likewise, for some equipment configurations, a reduced  $\varphi$  could be applicable based on manufacturers testing.

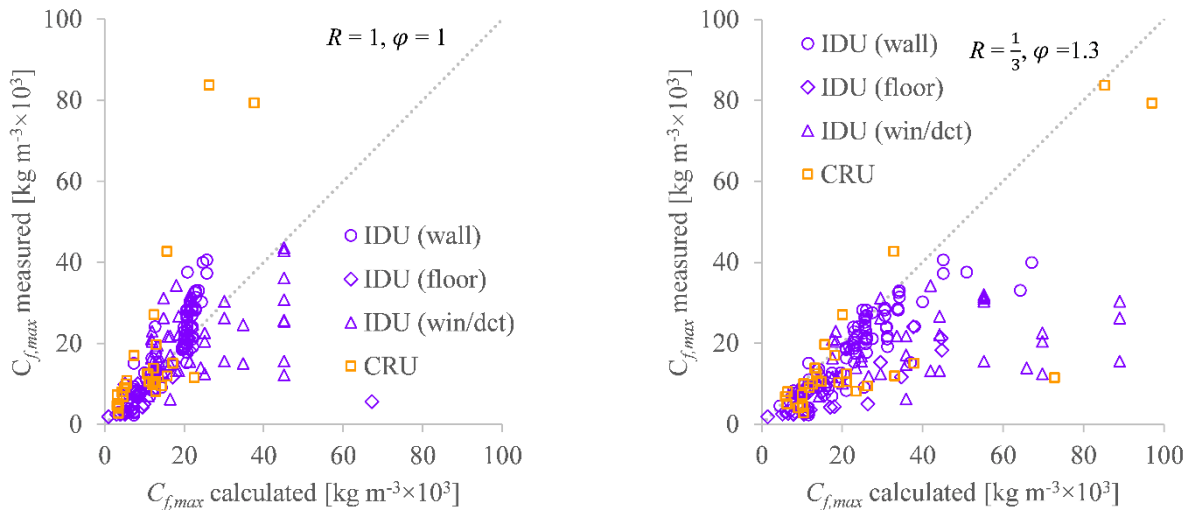


Figure 7: Comparison of measured  $C_{f,max}$  and unadjusted proposed formulae (left) and adjusted proposed formulae (right)

Further tests were carried out, at DMT/TÜV Nord (a safety institute), with wall IDUs and R290 concentrations measured at 20 sampling positions throughout the room. Over 50 tests were conducted with airflow rates set according to equation (19), in which both  $R$  and  $\varphi$  were applied. In addition to release mass flow, IDU height, airflow discharge angle (horizontal and downwards at  $-45^\circ$ ) and release mass, discharge opening area was also varied (100%, 66% and 33% of original area).

Figure 8 presents measured  $C_{f,max}$  against IDU airflow rates, where many of the data-points are well below LFL, indicating validity of the equation (19). Despite downwards airflow for some of the cases effectively

shortening  $x_T$ ,  $C_{f,max}$  is still below LFL, which is likely due to turbulent impingement as the jet hits the floor. The only arrangements leading to  $C_{f,max}$  exceeding LFL were IDUs positioned at 0.5 m, likely due to the Coandă effect (Etheridge and Sandberg) drawing the jet closer to the floor. Accordingly the formula could be adjusted to provide greater airflow for lower IDU positions. This was handled by introducing an adaption coefficient of  $\psi = 2$ , an index to  $h_a$  in equation (19), essentially representing a modification to Etheridge and Sandberg's analytical trajectory of  $x_T$  (equation 4).

Using  $\psi > 1$  compensates for air jets emanating at lower  $h_a$  which are drawn closer to the floor by increasing flow rate to enhance dilution. This increases  $\dot{V}_{o,min}$  by approximately 10%, which from analysis is deemed sufficient to bring all the data points to below LFL. Whilst the lowest IDU air discharge height of 0.5 m was used, only some RACS (e.g., packaged terminal AC,) may be installed so close to the floor. But air discharge with such units is upwards and above the air inlet such that low horizontal airflow parallel to the floor does not occur.

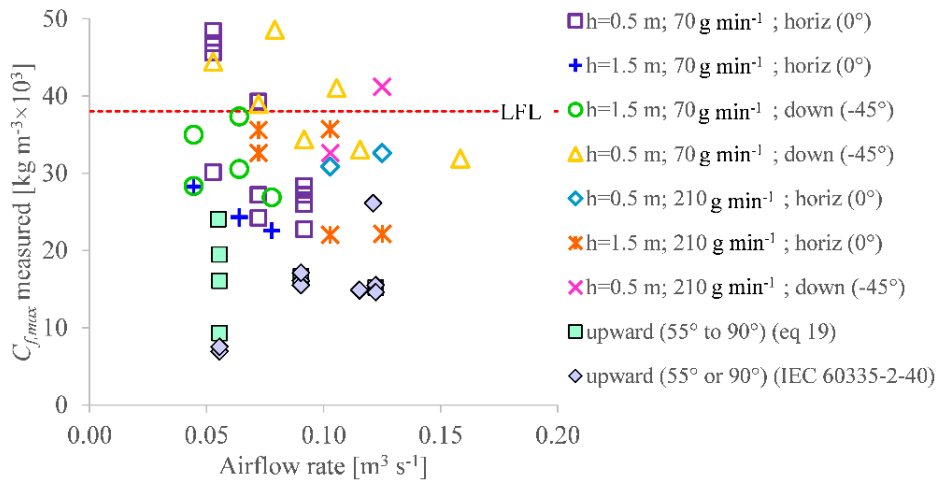


Figure 8: Measured  $C_{f,max}$ , where filled markers are for floor IDU with upward discharge and airflow using equation (19) or from IEC 60335-2-40

The overall revision of equation (19), including the application of heterogeneity term,  $R = \frac{1}{3}$ , adjustment factor,  $\varphi = 1.3$  and adaption coefficient  $\psi = 2$ , yields equation (20).

$$\dot{V}_{o,min} = \frac{5.4\sqrt{A_o}\dot{m}_{leak}^{3/4}}{h_a^{1/4}[LFL_m(1-F)]^{5/8}} \quad (20)$$

Tests with floor IDUs were included in Figure 8 (filled markers). These involved using airflow rates from equation (19) and also the minimum airflow calculated from IEC 60335-2-40 (clause GG.2.3.1; currently limited to “A2L” refrigerants). Floor IDU air discharge was at 0.66 m height and blowing either vertically upwards (90°) or at 55°, with released mass ranging from 0.25 kg to 0.85 kg at 70 g min<sup>-1</sup> to 200 g min<sup>-1</sup> in a 44 m<sup>3</sup> room. None of the cases resulted in  $C_{f,max}$  exceeding 70% of LFL, confirming that equation (19) can be suitably applied to IDUs with upwards airflow and that clause GG.2.3.1 can also be applied to R290.

Whilst equation (19) leads to unnecessarily high airflow, it allows the entire room volume to be considered for the mixing of the release (as opposed to a fraction of it), thus enabling a larger  $m_{ACL}$ ; it offers a more versatile approach.

Whilst the development and testing were based on R290, Colbourne and Suen (2018b) assessed the formulae for use with other flammable refrigerants, including those with much higher densities. It was concluded that the proposed formulae were applicable to all common flammable refrigerants.

#### 4 Initiation of airflow

A leak could occur when fans are not in operation and some form of leak detection may be employed to initiate the airflow to disperse the refrigerant. Two important factors need to be considered in relation to the dispersion of stratified mixtures: (i) initiation period of airflow (IPA) from start of the leak and (ii) maximum safe leak rate (MSLR) for sensors to respond to. To gain insight on these issues, further experiments were conducted using floor and wall IDUs.

##### 4.1 Initiation period of airflow

There is usually a delay in activating airflow once a leak establishes, during which a stratified layer may form on the floor and it is thus necessary to assess how effectively  $\dot{V}_{o,min}$  is able to disperse the mixture. Sample results (Figure 9) show concentrations at various floor locations in front of the IDU, where initiating the airflow respectively, 120 s and 80 s after commencing the R290 release decreases layer concentrations from  $1.5 \times \text{LFL}$  to below LFL in  $< 15$  seconds. Downward directed airflow is more effective than horizontal (as reflected by relatively more even distribution), despite the release mass flow being higher. This suggests that detection could also be used (if functionality permits) to favourably adjust discharge louver positions.

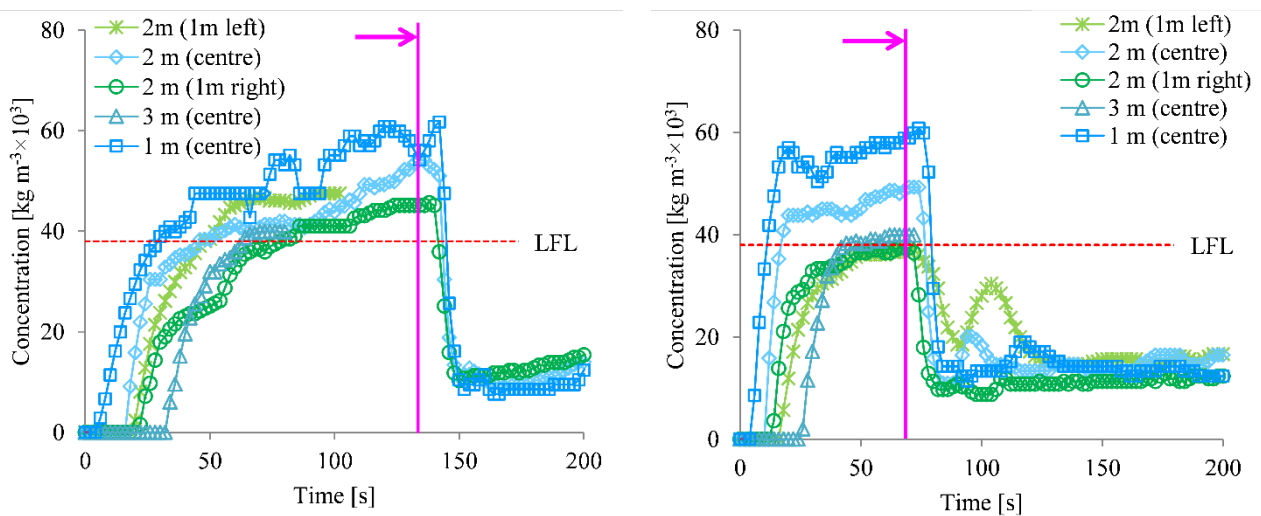


Figure 9: Effectiveness of airflow in mixing stratified layers. IDU at 1.0 m with airflow at  $0.19 \text{ m}^3 \text{ s}^{-1}$  directed downwards, mass flow of  $150 \text{ g min}^{-1}$  (left) and IDU at 1.0 m with horizontal airflow at  $0.19 \text{ m}^3 \text{ s}^{-1}$  and mass flow of  $90 \text{ g min}^{-1}$  (right). Arrows indicate the time at which the IDU fan is initiated



To determine the maximum delay permitted from start of the leak to initiating airflow, i.e., IPA, an approach was developed based on the time taken to build up an “intolerable” mixture volume in absence of airflow. This volume ( $V_{NE}$ ) was taken to be  $0.1 \text{ m}^3$  of mixture above 50% of LFL; referred as a “zone of negligible extent (NE)” (IEC 60079-10-1). Initiated airflow ensures the formation of this intolerable mixture volume is avoided.

IPA is taken as the sum of the three time elements:  $t_{IDU}$  being the duration between start of the release and when refrigerant emerges from the IDU,  $t_{dp}$  for the plume to descend from the IDU to the floor and  $t_{pf}$  for propagation across the floor until  $V_{NE}$  is formed.  $t_{IDU}$  depends upon the IDU configuration and release internal location but  $t_{IDU} = 3 \text{ s}$  is representative of the equipment involved in the present work.  $t_{dp}$  is dictated by IDU height and was found to be approximately 5 s per m.

For  $t_{pf}$ , a series of measurements were made. Sensors were positioned along the room floor centreline at 0.3 m increments to track the propagation of the R290 front. Figure 10 shows time taken for the front to travel beyond the first sampling point, for two different IDUs under a range of release mass flow rates. Time taken for the moving front (based on  $0.019 \text{ kg m}^{-3}$ , 50% of LFL) slows further from the release, indicating the propagation speed is decreasing, and as expected higher mass flows result in greater speeds. For the same mass flow rate, the front originating from wall IDU is about twice the speed of that from the floor IDU, due to greater momentum generated by the plume descent. This difference diminishes with higher mass flows.

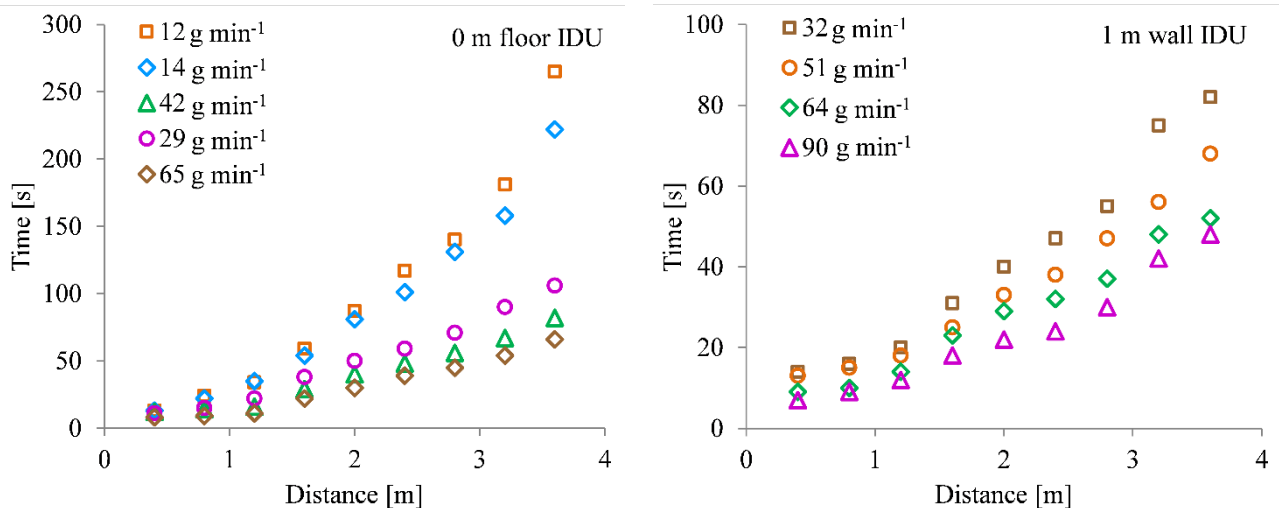


Figure 10: Mixture front travel time for different mass flow releases for 0.2 m floor IDU and 1.0 m wall IDU, based on a front concentration of  $0.019 \text{ kg m}^{-3}$

The average front propagation speed ( $\bar{u}_{pf}$ ) against mass flow rate is presented in Figure 11. It is assumed that the flow spreads in a semi-circular fashion, with a layer height,  $h_l = 0.5 \text{ m}$  for the wall IDU and  $h_l = 0.2$

m for the floor IDU (from Colbourne and Suen, 2021). The time taken to reach  $V_{NE}$  was estimated from

$$t_{pf} = \frac{\sqrt{2V_{NE}/\pi h_l}}{\bar{u}_{pf}}, \text{ as also presented in Figure 11.}$$

Accordingly,  $t_{IPA}$  can be calculated from equation (21),

$$t_{IPA} = t_{pf} + 5h_o + 3 \quad (22)$$

where  $h_o$  is the unit base height and using a curve-fit,  $t_{pf} = \frac{1}{a_1 \ln \dot{m}_{leak} + a_2}$ ,  $a_1 = 0.025$  and  $a_2 = 0.23$ .

Application of IPA is primarily associated with the design of the leak detection system. For instance, practical testing would indicate whether modifications are needed to the type of sensor and/or its response time, its positioning within the equipment and even the internal configuration of piping and channels within the IDU. Such modifications should be carried out until testing demonstrates that from initiation of the simulated leak to the fan delivering  $\dot{V}_{o,min}$  the time is no more than  $t_{IPA}$ . In practice,  $t_{IPA}$  should be independent of the room the unit is installed in because  $V_{NE}$  will be reached before the mixture has spread to the room walls.

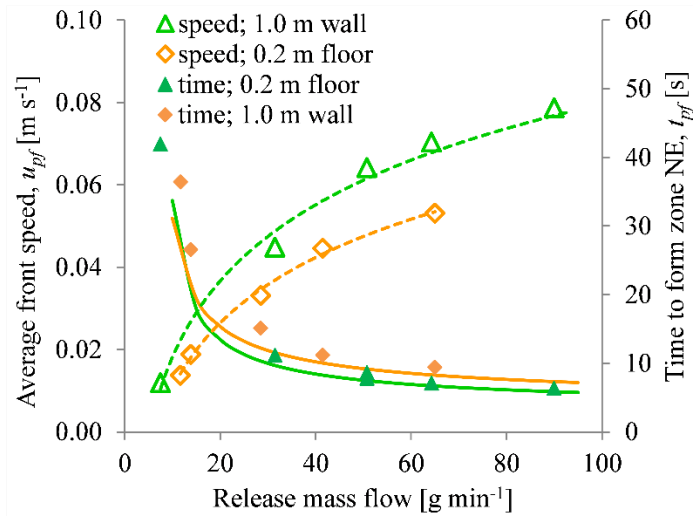


Figure 11: Average propagation speed of a  $0.019 \text{ kg m}^{-3}$  mixture front along the floor and  $t_{pf}$

#### 4.2 Maximum safe leak rate

Whilst a very slow refrigerant leak into a quiescent room will unlikely form a flammable mixture, a faster leak may. Therefore, an approach is needed to identify MSLR so that when reaching this leak rate, the detection system needs to activate  $\dot{V}_{o,min}$ . Measurements under quiescent conditions show  $C_{f,max}$  is broadly related to release height (assumed equal to  $h_o$ ) and room area, so MSLR can be estimated by equation (23).

$$\dot{m}_{MSLR} = \vartheta h_o A_{rm} LFL \quad (23)$$

where  $\vartheta$  is an experimentally determined constant that encompasses  $F$  and release duration.

To determine  $\vartheta$ , IDUs were positioned at four different heights ( $h_o = 0.5$  m, 1.0 m, 1.5 m and 2.0 m) and releases of R290 were made at incrementally greater mass flow rates, up to  $m_{ACL}$  from equation (18) and a  $F$  of 0.5. Figure 12 presents  $C_{f,max}$  over a range of mass flow rates. When  $C_{f,max} = \text{LFL}$  (using interpolation of best-fit curves), the corresponding mass flow rate was then applied to equation (23). For each  $h_o$ , all  $\vartheta$  were determined to be to within  $\pm 3\%$  of  $0.00033$   $\text{s}^{-1}$ .

When testing response of a leak detection system, the simulated leak uses MSLR to ensure the airflow will provide  $\dot{V}_{o,min}$  within IPA.

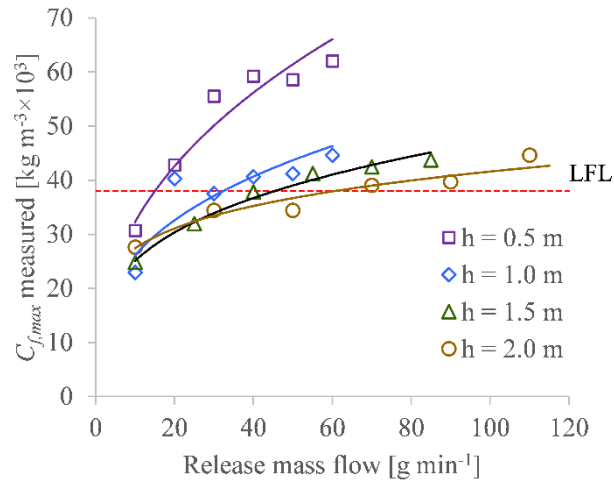


Figure 12: Variation of  $C_{f,max}$  over a range of release mass flow rates and unit heights

## 5 Sample outputs and discussion

Using equation (20) with R290, minimum IDU airflow rates are estimated for RACS (Table 2), with a room area ranging from 10 to 50  $\text{m}^2$  assuming 200  $\text{W m}^{-2}$  specific heat load and a release mass flow corresponding to  $m_{ACL}$  over 4 minutes or  $60$   $\text{g min}^{-1}$ .

Having the IDU positioned at 1 m is observed to demand an additional 20% higher airflow compared to those at 2 m. For  $F = 0.25$ ,  $\dot{V}_{o,min}$  with  $\dot{m}_{leak} = m_{ACL} \div 4$  minutes, is generally smaller than the typical IDU highest airflow setting but greater than lowest setting, suggesting that most products would be able to disperse the leak. With  $F = 0.50$ ,  $\dot{V}_{o,min}$  is nearly always greater than the highest airflow setting, suggesting some products may need to have highest airflow settings increased. With  $\dot{m}_{leak} = 60$   $\text{g min}^{-1}$ ,  $\dot{V}_{o,min}$  is mostly below the lowest airflow setting, regardless of  $F$ .

IPA is dependent upon IDU height and release mass flow but does not vary significantly, suggesting the use of a single value could be appropriate. Values of MSLR are greater for larger room sizes and higher IDUs, but independent of  $F$ , implying less sensitive detection systems could be employed for larger RACS.

Table 2: Example of calculated minimum and typical airflow rates

$A_{rm}$ [m <sup>2</sup> ]	$Q$ <sup>a</sup> [kW]	$F$ [-]	$h_o$ [m]	$m_{ACL}$ , eq. (18) [kg]	Typical $\dot{V}$ low <sup>c</sup> [m <sup>3</sup> s <sup>-1</sup> ]	Typical $\dot{V}$ high <sup>c</sup> [m <sup>3</sup> s <sup>-1</sup> ]	$\dot{V}_{o,min}$ , eq. (20) <sup>d</sup> [m <sup>3</sup> s <sup>-1</sup> ]	$\dot{V}_{o,min}$ , eq. (20) <sup>e</sup> [m <sup>3</sup> s <sup>-1</sup> ]	$t_{IPA}$ , eq. (22) <sup>d</sup> [s]	$t_{IPA}$ , eq. (22) <sup>e</sup> [s]	$\dot{m}_{MSLR}$ , eq. (23) [g min <sup>-1</sup> ]
10	2	0.25	1	0.21	0.042	0.083	0.044	0.049	26	25	8
20	4	0.25	1	0.42	0.083	0.167	0.104	0.069	22	25	15
30	6	0.25	1	0.63	0.125	0.250	0.173	0.085	20	25	23
40	8	0.25	1	0.84	0.167	0.333	0.248	0.098	19	25	30
50	10	0.25	1	1.05	0.208	0.417	0.328	0.109	18	25	38
10	2	0.25	2	0.21	0.042	0.083	0.037	0.041	31	30	15
20	4	0.25	2	0.42	0.083	0.167	0.088	0.059	27	30	30
30	6	0.25	2	0.63	0.125	0.250	0.146	0.072	25	30	45
40	8	0.25	2	0.84	0.167	0.333	0.209	0.082	24	30	60
50	10	0.25	2	1.05	0.208	0.417	0.276	0.092	23	30	75
10	2	0.5	1	0.42	0.042	0.083	0.095	0.063	22	25	8
20	4	0.5	1	0.84	0.083	0.167	0.226	0.089	19	25	15
30	6	0.5	1	1.25	0.125	0.250	0.376	0.109	18	25	23
40	8	0.5	1	1.67	0.167	0.333	0.538	0.126	17	25	30
50	10	0.5	1	2.09	0.208	0.417	0.712	0.141	17	25	38
10	2	0.5	2	0.42	0.042	0.083	0.080	0.053	27	30	15
20	4	0.5	2	0.84	0.083	0.167	0.191	0.075	24	30	30
30	6	0.5	2	1.25	0.125	0.250	0.316	0.091	23	30	45
40	8	0.5	2	1.67	0.167	0.333	0.453	0.106	22	30	60
50	10	0.5	2	2.09	0.208	0.417	0.599	0.118	22	30	75

<sup>a</sup> Based on 200 W m<sup>-2</sup> room floor area; <sup>b</sup>  $A_o = 0.015 \times Q$ , <sup>c</sup> lowest  $\dot{V} = 0.021 \times Q$ , highest  $\dot{V} = 0.042 \times Q$  (derived from product catalogues), <sup>d</sup>  $\dot{m}_{leak} = 1000 \times m_c / 4$  g min<sup>-1</sup>, <sup>e</sup>  $\dot{m}_{leak} = 60$  g min<sup>-1</sup>

## 6 Final remarks

An extensive programme of experimental work was conducted to understand the processes involved in the dilution of a refrigerant leak from IDUs when airflow is present. Data and observations acquired were used to help derive semi-empirical formulae for estimating minimum airflow rates to greatly minimise the possibility of reaching flammable concentrations within the room in the event of a leak; however, absolute avoidance of potentially hazardous situations is not possible (Colbourne and Suen, 2004).

Application of the formulae was checked against experiments using wall and floor IDUs and CRUs, including for the case where initiation of airflow is delayed as a leak forms a stratified layer. Although the

study used R290, accompanying work demonstrated the approach was equally applicable to all other flammable refrigerants. Further, formulations were provided to estimate MSLR for when airflow is needed and IPA for determining suitable response time for a detection system.

The proposed equations are practical and easy to use as judgements on certain variables are not needed, and discharge velocity, refrigerant charge, air discharge height and choice of assumed leak mass flow rate are all accounted for. IDU and CRU can easily be assessed to determine whether they provide sufficient airflow to prevent formation of LFL on room floors. This formula represents a major improvement to the minimum airflow requirements for equipment using flammable refrigerants specified within RACHP safety standards.

### **Acknowledgements**

The authors would like to acknowledge project Proklima of the Deutsche Gesellschaft für Internationale Zusammenarbeit (GIZ) GmbH, HEAT GmbH, Deutsche Umwelthilfe e.V., Environmental Investigation Agency International (EIA) and the EU LIFE FRONT Project for supporting this work.

### **References**

1. Colbourne, D., Pitarch Mocholi, M., Munzinger, P., Oppelt, D., Paetzold, B., Vince, I. 2021b. Leak hole sizes from refrigeration, air conditioning and heat pump systems. *Int. J. Refrig.*, doi.org/10.1016/j.ijrefrig.2021.07.003.
2. Colbourne, D., Suen K. O. 2004. Appraising the flammability hazards of hydrocarbon refrigerants using quantitative risk assessment model. Part II. Model evaluation and analysis. *Int. J. Refrig.* Vol. 27, no. 7, pp. 784-793, DOI: 10.1016/j.ijrefrig.2004.07.002
3. Colbourne, D., Suen, K. O. 2018a. Minimum airflow rates to dilute R290 concentrations arising from leaks in room air conditioners. Proc. 13th IIR Gustav Lorentzen Conference on Natural Refrigerants (GL2018). Valencia, Spain
4. Colbourne, D., Suen, K. O. 2018b. Minimum airflow rates to dilute A2L refrigerant leaks from refrigeration systems. Proc. 1st IIR international conference on the application of HFO refrigerants, Birmingham, UK.
5. Colbourne, D., Suen, K. O. 2021. Hydrocarbon refrigerant charge limits for quiescent rooms. *Int. J. Refrig.*, vol. 125, pp. 75–83.
6. Colbourne, D., Suen, K.O., Li, T.-X., Vince, I., Vonsild, A., 2020. General framework for revising class A3 refrigerant charge limits –a discussion. *Int. J. Refrig.* doi: 10. 1016/j.ijrefrig.2020.04.024, <https://doi.org/>.
7. Doll, U., Stockhausen, G., Willert, C. 2017. Pressure, temperature and three-component-velocity fields by filtered Rayleigh scattering velocimetry. *Optics Letters* 1 DOI:10.1364/OL.42.003773
8. Etheridge, D., Sandberg, M. 1996. Building ventilation: theory and measurement. British Gas Research and Technology, John Wiley & Sons, UK.
9. Hu, M., Li, J., Liu, Z., Li T. 2018. Experimental and numerical simulation analysis of R-290 air conditioner leak. *Int. J. Refrig.* 90 163–173.
10. IEC 60079-10-1: 2021. Explosive atmospheres. Classification of areas – Explosive gas atmospheres.
11. IEC 60335-2-40: 2017. Household and similar electrical appliances – Safety – Part 2-40: Particular requirements for electrical heat pumps, air-conditioners and dehumidifiers.
12. Jia, L., Jin, W., Zhang, Y. 2015. Analysis of indoor environment safety with R32 leaking from a running air conditioner. *Procedia Engineering* 121 (2015) 1605 – 1612.

13. Jin, W., Gao, P., Zheng, Y. 2017. Experimental study on ventilation effect on concentration distribution of R32 leaking from floor type air conditioner. *Energy Procedia* 105 (2017) 4627 – 4634.
14. Morton, B. R., Taylor, G. I., Turner, J. S. 1956. Turbulent gravitational convection from maintained and instantaneous sources. *Proc. R. Soc. Lond. A* 234, 1-23, <https://doi.org/10.1098/rspa.1956.0011>
15. Ram Prakash, C., Gautham, M. R., Mohan Lal, D., Devotta, S., Colbourne, D. 2021. CFD Simulation of HC-290 leakage from a split type room air conditioner. *Proc IMechE Part E: J Proc. Mech. Eng.*, DOI: 10.1177/09544089211021274J
16. Turner, J. S. 1986. Turbulent entrainment: the development of the entrainment assumption, and its application to geophysical flows. *J. Fluid Mech.*, vol. 173, pp. 431-471